SEEJPH 2024 Posted: 00-00-2024

Experimental and DFT Study of Structural and Electronic Properties of Polyfuran@nanoCuO Hybrid Polymer

Saddiq H. Abbas[1*], Salah S. Al-Luaibi[1*], Bahjat A. Saeed[2]

[1,2]*Department of Chemistry, College of Science,*
[3]*Department of Chemistry (College of Education for Pure Sciences). University of Basrah, Iraq*
**For the Corresponding author: Email address sadiqq8119@gmail.com*
***Corresponding author, Email address: salah.hashim@uobasrah.edu.iq*
****Corresponding author, Email address: bahjat.saeed@hotmail.com*

KEYWORDS

(PFu @CuO NPs), Energy band gap Computational investigation, DFT

ABSTRACT

Polyfuran (PFu) and polyfuran combined with copper oxide nanoparticles (NPs) 25 nm to form (PFu@CuO) were synthesized using oxidation polymerization in the presence of FeCl3 and core-shell polymerization methods. The effective synthesis of PFu@CuO and the dynamics of interaction between PFu and CuO NPs were corroborated through a diverse range of characterization techniques, including field emission scanning electron microscopy (FESEM) and X-ray diffraction (XRD) analysis, which elucidated the crystalline transformation of PFu in association with CuO(NPs). The vibrational modes were meticulously examined via infrared spectroscopy. UV-VIS absorption spectra were acquired, and the energy band gap was computed, demonstrating a reduction from 2.51 eV for unmodified PFu to 1.49 eV for PFu@CuO, as elucidated through the Tauc plot. The thermal characteristics were evaluated through thermogravimetric analysis (TGA). A theoretical investigation was executed to ascertain the adhesion energy of the polymer on the nano-metal oxide surface, employing the Material Studio software. Computational analyses, with a particular emphasis on PFu@CuO(NPs), systematically juxtaposed the properties of polyfuran with those of polyfuran adsorbed onto the nano-metal oxide surface. Molecular modeling, employing the COMPASS force field, clarified the intricate interactions between polymers and metal oxides, indicating an enhanced adhesion between polymer oligomers and metal oxides, which is crucial for the progression of polymer composite design. Additionally, computational evaluations of the molecular framework of polyfuran provided significant insights into its geometric, spectroscopic, and electronic properties, with density functional theory (DFT) calculations performed using the B3LYP/6-311G++ (d, p) basis set revealing a relationship between the oligomer count and the energy gap. Furthermore, molecular dynamics simulations were conducted to ascertain the glass transition temperature and to compare it with the experimentally determined glass transition temperature, as well as to evaluate the degree of compatibility between practical and theoretical aspects, thereby demonstrating the substantial capacity of molecular dynamics simulation methodologies in exploring the morphology of polymers and improving their functional characteristics**.** This comprehensive study advances our understanding of polymer-metal oxide interactions and informs the design of tailored polymer composites with enhanced functionality.

1. Introduction

Metal and metal oxide-containing polymers have gained more attention because of their potential applications. It can be an amalgamation of metals, which can modify the basic bulk properties of these polymers, such as thermal, insulation, conductive stability, and other physical and chemical properties. In general, the thermal stability of metal-containing polymer systems is Relatively enhanced compared to the bulk Polymer [1-2] Moreover, the coordination ability of the metal inside the polymer backbone allows these materials to serve as sensors and as building blocks for supramolecular structures (7). Also, the metal part can Be incorporated into the polymer backbone by either covalently linking directly to the main chain or coordinating with links within the spine. [3] . Organic electronics has developed rapidly over the past period Two decades [4]. This was partly driven by progress in synthetic chemistry, which allowed the creation of. New conjugated materials with customized properties. Is used for Conjugated materials cover a wide range of applications, including sensors [5] . dyes, organic photovoltaics (OPVs), [6] . organic field effect transistors (OFETs) [7] and organic light-emitting diodes (OLEDs). [8]. Furan, the oxygen homolog of thiophene, is relatively unrepresented in the literature, although its properties and enthusiasm make it desirable for use in conjugated systems. [9]. In recent years, flexible devices have posed a new challenge for electronics and optical fields, so extensive investigations have been conducted on conducting polymers with functionalization. Special characteristics of electronic slander. Due to smaller resonance energy, devices containing compounds based on conjugated heterocyclic aromatic rings, such as pyrrole and furan, showed good efficiencies. [10-11].The pairing of electronic engineering occurred. Synthesis of organic materials urges researchers to make significant progress in the performance of conjugated materials for electronic applications. [12-13] . The conjugated and electrically conductive polymer field still attracts much scientific and technological interest. [14]. Among them, an

important class of heterocyclic polymers, poly furans PFu, has rarely existed. It has been explored but not proven as a conductive polymer. This is due to the low difficulty of polymerization Stability and weak properties of poly furan samples Obtained.5 reported electrical connections The doped Pfu was measured in the range of 10^5 to 10^2 S cm^{-1}. [15] . Polyfuran has also been reported to be environmentally friendly. Electrochemically unstable. Furan (Fu) is an aromatic heterocyclic ring composed of C_4H_4O. Polyfurans are arrangements of furan rings with different configurations. Functional theory (DFT) has recently been essential for theoretical studies of organic molecules and related fields, such as studying the behaviors of polymers. Besides, the DFT approach is an extremely important and useful tool for exploring the relationship between geometry and electronic properties Of a chemical compound [16-17]. such as DFT calculations of the highest occupied molecular orbital (HOMO) - lowest unoccupied Molecular orbital energy (LUMO) with different chemical reaction parameters, and energy gap calculation.

2. Methodology

Sourcing and preparation of Core-shell polymer

Furan (Sigma-Aldrich) was used after double distillation, CuO nanoparticle (NPs)(nanopowder, 25 nm particle size). Anhydrous ferric chloride ($FeCl_3$), chloroform, and methanol were purchased from Merck. And ultrasonic bath.

Experiments

Chemical Synthesis of Polyfuran (Pfu)

The required quantity of furan monomer (1 mole) is dissolved in a suitable solvent, specifically 25 ml of chloroform $CHCl_3$. while utilizing magnetic stirring for 5 minutes. Concurrently, an equivalent amount of FeCl3 (1 mole) is dissolved in 25 ml of chloroform and subjected to magnetic stirring for the same 10 min interval. The oxidizing agent is introduced progressively, in a dropwise manner, into the furan reaction mixture, which is thereafter sustained under magnetic stirring for an extended duration (typically 24 hours) at ambient temperature to promote the completion of the oxidative polymerization process. The change in hue detected in the resultant mixture denotes the successful formation of polyfuran. Subsequently, the precipitate is separated through filtration employing a Buchner funnel to obtain the synthesized polyfuran, and Dry the polyfuran in a vacuum oven or dryer at a low temperature 60 ℃ until a stable weight is achieved. which is subsequently rinsed with methanol and deionized water to remove any. [18].

Core-shell polymerization Pfu@ CuO

The necessary amount of the composite, consisting of 1 mole of furan monomer and 10%(w/w) of copper oxide nanoparticles(CuO NPs), must be dissolved in an appropriate solvent, employing 25ml, in 25 ml of chloroform $CHCl_3$ with the assistance of an ultrasonic bath to attain a uniform dispersion over 30 min. Simultaneously, 1mole of $FeCl_3$ is required to be dissolved in 25 ml of $CHCl_3$ and subjected to stirring for 10 min; thereafter, the oxidizing agent is to be incrementally incorporated into the mixture, which is sustained under magnetic stirring for a prolonged duration, typically 24 hours, at ambient temperature to promote the completion of oxidative polymerization. A change in color to a deep brown precipitate will indicate the successful formation of the hybrid polymer, identified as PFu@CuO NPs. Subsequently, the precipitate ought to be filtered employing a Buchner funnel to separate the synthesized polyfuran; the precipitate should be meticulously washed with methanol and deionized water to remove any residual unreacted ferric chloride, after which the polyfuran is to be subjected to drying in a vacuum oven or dryer at a precisely regulated low tempe of 60 ℃ a stable mass is achieved [19].

Characterization and evaluation

FT-IR analysis

Every spectrum was recorded in a frequency range of 400 to 4000 cm^{-1} using a potassium bromide

(KBr) tablet. Pre-oven dried. [20-21]. FT-IR spectra of CuO nano, PFu, and Pfu@CuO are shown in Fig (1 a,b and c). The bands in the FTIR spectrum represent the vibrations of CuO nanoparticle bonds located between 871,589 and 475 cm^{-1}. CuO nanoparticles' spectra shows a distinct peak at 589 cm^{-1}, which indicates the production of Cu-O bonds. Because nanocrystalline materials have a high surface-to-volume ratio and can thus absorb moisture, the broad absorption peak at about 3393 cm^{-1} is caused by adsorbed moisture. [22-23]. The spectral feature of pure PFu is well-known in the literature [24] In the PFu spectrum, peaks are located around 1026 cm^{-1}: C–O–C stretching vibration, C = C Stretching vibrations, and out-of-plane bending vibrations C-H, respectively. Moreover, the peaks are at 1211, 736,798, And 3279 cm^{-1} for the interposition Furan rings, carbonyl stretching, and vibrational mode on the ether C-H Stretching vibration [25]. and hydroxyl groups, respectively, at 3626-3518. The presence of these bands confirms the formation of PFu. In the FT-IR spectrum of PFu@CuO, broadband at 3439 cm^{-1} can be assigned to O-H vibration and peak At 435-462 cm^{-1}, corresponding to the CuO stretching mode [26-27].

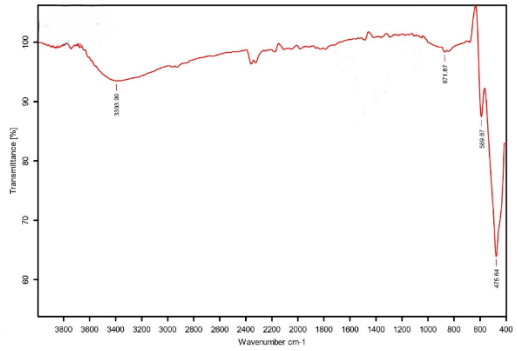

Fig. (1a) FT-IR spectra of CuO nanoparticle

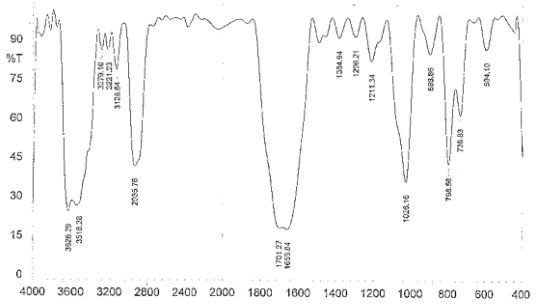

Fig.(1b) FT-IR spectra of Pfu

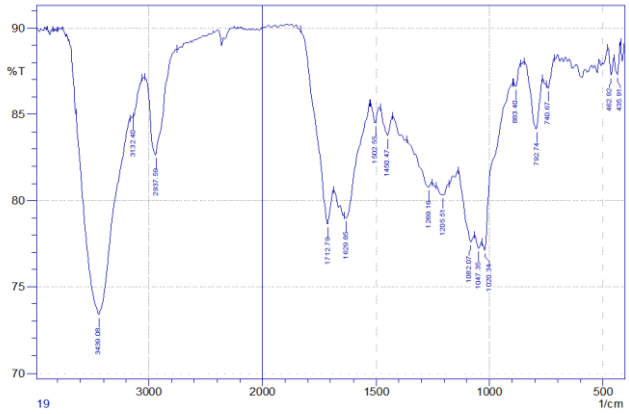

Fig.(1c) FT-IR spectra of Pfu@CuO

3.2. XRD Analysis

The XRD was used to study the crystallinity and particle size of the Pfu@CuO. Fig. (2a) shows the XRD patterns of PFu. Only one broad peak is centered near the value 2θ=17° corresponding to the amorphous character of PFu. In the XRD pattern of Pfu@CuO, five distinct peaks appear, as shown in the fig. (2b). The diffraction patterns appeared at 2θ values (18°, 65) assigned to the (001), (2 2 0) levels of CuO nanoparticles, respectively. The crystalline nature of Pfu@CuO may have been improved due to the interaction of PFU and CuO nanoparticles. The average diameter of Pfu@CuO was calculated from the Scherer equation Eqn. 1. Our results showed that according to the Scherer equation, the average crystal size reached 56.2 and 52nm, respectively, indicating the interaction between the polymer and the crystalline surface of the nanoparticles [28].

$$D = \frac{K.\lambda}{\beta.cos\,\theta} \quad \ldots\ldots\ldots \text{Eqn. 1}$$

Where: D is the average crystallite size in the direction perpendicular to the lattice planes, K is a numerical factor frequently referred to as the crystallite-shape factor, λ is the wavelength of the X-rays,

$\beta$is the width of the X-ray diffraction peak in radians, and θ is the Bragg angle.

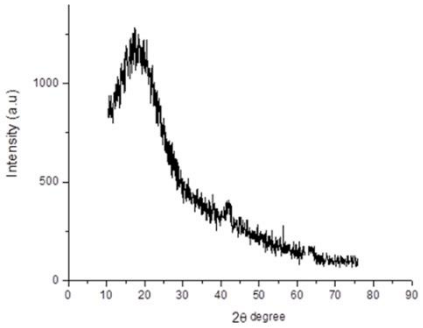

Fig. (2a) shows the XRD patterns of Pfu

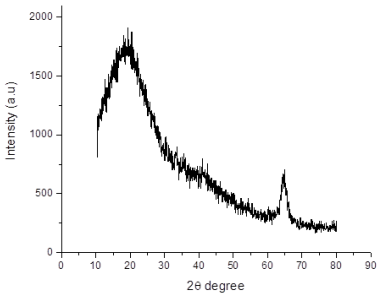

Fig. (2b) The XRD patterns of Pfu@CuO

FESEM Analysis

FESEM is one of the most widely used techniques in the morphological study of polymeric materials to analyze their composition and texture. Fig. (3a) shows FESEM images of polyfuran, which shows an amorphous structure with a particle size of about 56 - 52 nm. As for Fig.(3b), FESEM images of PFU@CuO show a spherical particle morphology. The particle sizes of PFU@CuO are 52 to 48 nm [29].

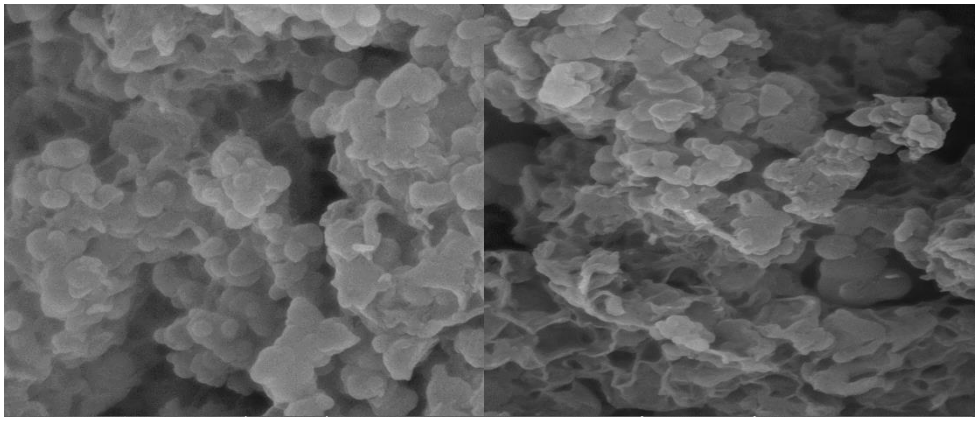

Fig. (3a) FESEM images of Pfu.

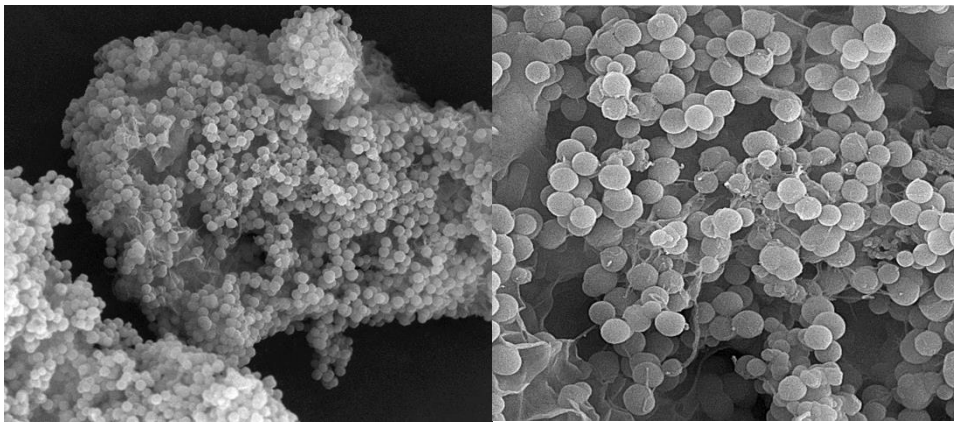

Fig. (3b) FESEM images of PFU@CuO.

Thermal Analysis

The prepared samples were analyzed using an SDT Q600 V20.9 Build 20 thermal analyzer with a heating rate of 20°C/min using an inert nitrogen atmosphere. Figure (4) represents the TGA curve. The initial temperature (Ti) and final temperature (T_f) were recorded to evaluate the thermal stability of the polymer and the effect of nanosized copper oxide on the polymer structure and thermal stability. The max temperatures T_{max} and $T_{\%50}$ were also recorded. The remaining weight of the samples is shown in Table (1), where the effect of nanoparticles on the thermal stability of the polymer was measured. They are observed by calculating the activation energy using the Broido equation (2) used to obtain the activation energy (Ea). The presence of nano-metal oxide showed an effect by reducing the rate of thermal disintegration and the amount of residue. Thermal stability was observed through the high value of the activation energy of the hybrid polymer = 25.08 KJ.mol^{-1} compared to the activation energy of the polymer, which is equal to 24.3 KJ.mol^{-1}[30].

$$\ln[-lny] = -Ea/RT$$

Where:

$$y = w\circ - wt \ / w\circ - w\infty$$

Wo= the initial weight of the polymer, Wt = the weight of the residual polymer at any temperature W∞ = the final weight of the polymer remaining at the end of dissociation R = the gas constant T = the measured temperature when calculating Wt.

By drawing the relationship between In[-lny] and 1/T from the slope of the straight line, the activation energy can be calculated.

Table (1). Thermogravimetric Parameters of PFu, Pfu@nano CuO

Polymer	Decomp.Temp. C			50% wt loss %	Rate of decomp. %/C	Char content %	Activation energy kJ/mol
	T_i	T_{op}	T_f				
PFu	170	341	598	420	0.2	47.1	25.08
PFu@CuO	130	283	502	411	0.18	50.71	24.3

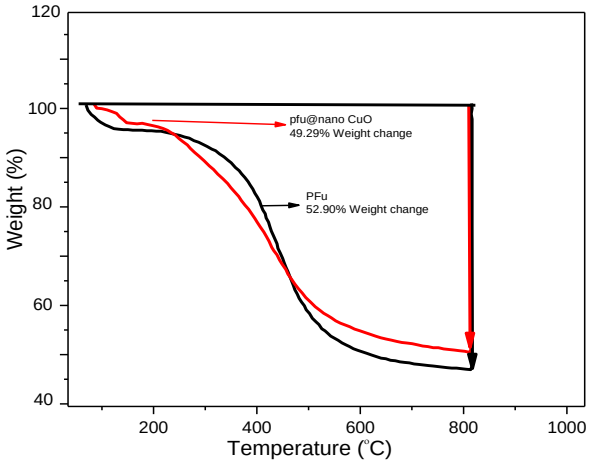

Fig (4) TGA thermograms of PFu and Pfu@ CuO

UV-Vis Analysis and Energy Band Gape Calculation

Studying and determining energy gap values is essential for understanding optical properties and parameters. The use of metal oxide nanoparticles influences the distribution and arrangement of

molecules within the polymer chain, affecting the energy gap (Eg) values. Table (2) illustrates the impact of metal oxide nanoparticles on the band gap. The energy gaps of pure PFu and PFu@CuO were investigated using absorption bands in the ultraviolet region, with Eg estimated via the Tauc equation Eqn.2[31]. The UV-visible spectra of PFu and PFu@CuO, shown in Figure (5), reveal two absorption peaks: the first peak at λ_{MAX} 438 nm, attributed to the π-π transition of the furan rings in the PFu backbone, and a second absorption peak at λ_{MAX} 497 nm. For PFu@CuO, absorption is observed in the n-π transition of the quinoid rings [32]. Comparing the UV spectra of PFu@CuO nanocomposites shows that the characteristic peaks for π-π and n-π transitions of the PFu@CuO polymer chain shift to longer wavelengths in the presence of CuO nanoparticles. This shift suggests an interfacial interaction between PFu and CuO nanoparticles (Jubu, Peverga R., et al., 2022). Additionally, a significant change in the energy gap was observed, with values calculated at 3.52 eV for PFu and 2.01 eV for PFu@CuO. These results indicate enhanced alignment of conjugated furan segments, which promotes charge flow through the nanocomposite matrix[33].

$(\alpha\ h\nu)^2 \propto (h\nu)$ ….. **Eqn.2**

Where α: the optical absorption coefficient, h is the Planck constant, ν is the photon's frequency, Eg is the bandgap energ

Table (2) shows the effectiveness of metal oxide nanoparticles on band gap

content	λ_{MAX}(nm)	The energy band gap (ev)
PFu	438	3.52
Pfu@CuO	497	2.01

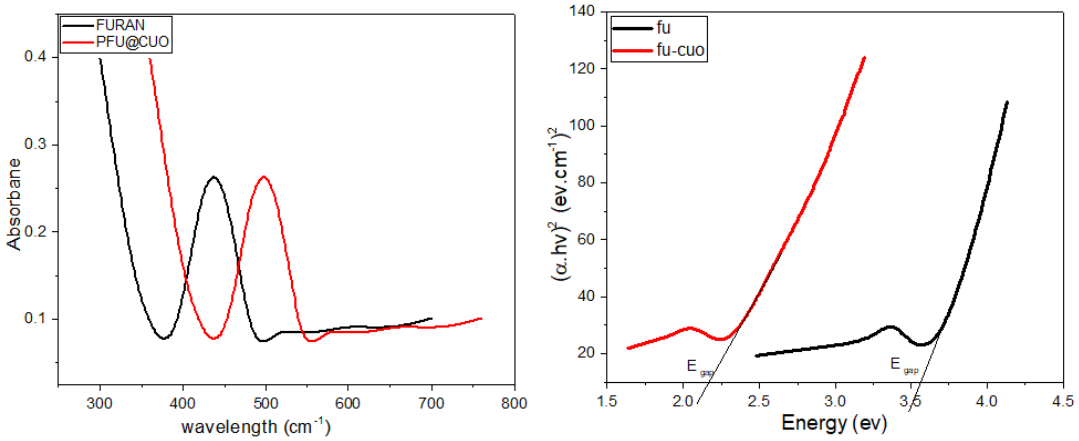

Fig. (5**)** UV.spectra and Energy gap of Pfu and Pfu@CuO

4. Interaction of polymers with metal oxides

This study provides a good idea of polymer and non-polymer interactions by purchasing molecular modeling. The force field in COMPASS is applied to simulations to calculate the interface. Fig. (6) shows the interaction between pfu and CuO nanoparticles, and a molecular dynamics approach is used to study the interaction and adsorption of PFu and CuO nanoparticles. On the other hand, as the results of theoretical calculations are shown in Table (3), investigations help explore polymer composites. Much better adhesion is achieved by calculations between the polymer oligomers and the metal oxides under study. The interaction or adhesion energy is calculated using Eqn.3 .to equal (-3660.6) kcal/mol. [34-35].

$E_{Interaction} = E_{total} - (E_{surface} + E_{polymer})$ ……. **Eqn.3**

This comprehensive analysis advances our understanding of polymer-metal oxide interactions and underscores the potential for designing advanced polymer composites with tailored properties and enhanced functionality.

Polymer @ Metal oxide Surface	$E_{surface}$ kcal/mol	$E_{polymer}$ kcal/mole.	$E_{surface} + E_{polymer}$ kcal/mol	$E_{total\ of\ layer}$ kcal/mol	$E_{interaction}$ kcal/mol
Polyfuran@nanoCuO	-721120.39	356.91	-720763.48	-724424.08	-3660.6

Table (3) shows the interaction energy of Polyfuran@nanoCuO

- The interaction energy of (pure polyfuran) = 356.91 kcal/mole.

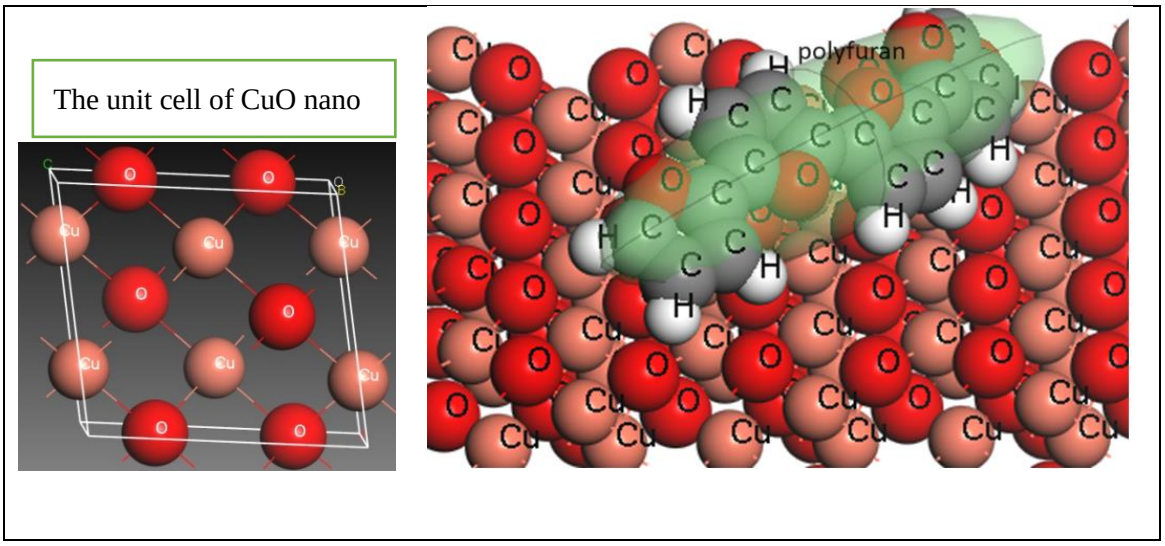

Fig.(6) shows the interaction between pfu and CuO nanoparticles

5. Computational details

The utilization of Density Function Theory (DFT) in the basis set with B3LYP/6-311G++ (d, p) was employed to examine the geometric, spectroscopic, and electronic characteristics of PF, yielding a noteworthy outcome. The determination of the energy gap involves the computation of the disparity between the estimations of electronic properties for HOMO and LUMO as shown in Scheme 1 , as indicated in Table (4). A correlation was established between the quantity of monomers and the energy gap, revealing a direct relationship where an escalation in the number of monomers results in a sequential increase and a decrement in the energy gap. The coefficient of determination, denoted as R2, was utilized to assess the proximity of the fitted data to the regression line. The significance of both correlation and regression in data analysis cannot be overstated. The coefficient of determination was identified as 0.9612, signifying the extent of variability in the dependent variable explained by the independent variable, approaching the values portrayed in the integers of Figure (7) [36-38].

Table (4) shows the values calculated according to the DFT for the energy gap by calculating the energies of HOMO and LUMO

No. monomer unit	HOMO	LUMO	E gape (ev)
1Fu	-5.187	-1.605	3.581
2Fu	-4.529	-2.310	2.219
3Fu	-4.01	-2.345	1.66
4Fu	-2.879	-1.341	1.537
5Fu	-3.763	-2.362	1.400
6Fu	-4.392	-3.082	1.309
7Fu	-4.498	-3.292	1.205
8Fu	-4.43	-3.233	1.196
9Fu	-4.417	-3.258	1.158

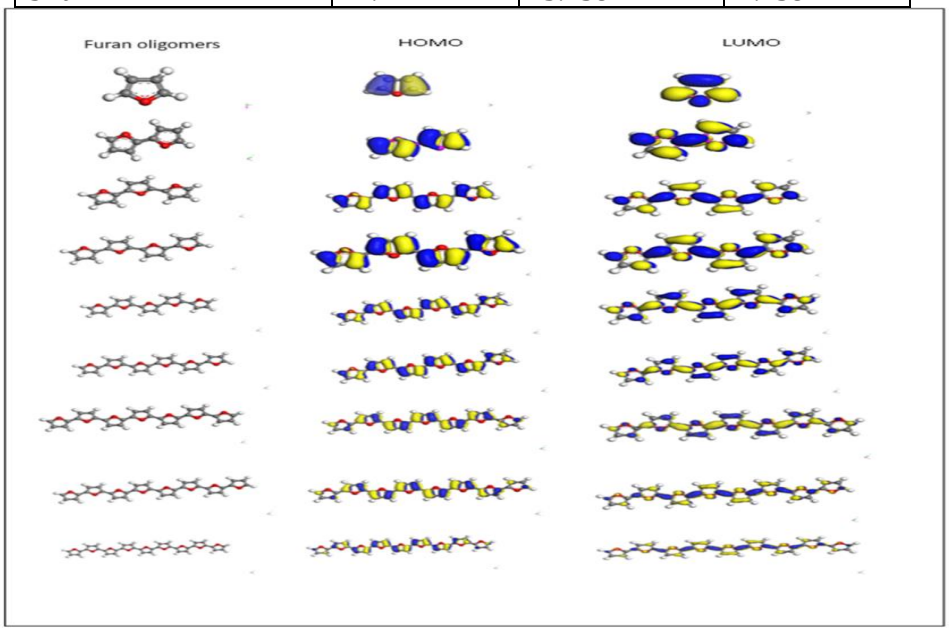

Scheme 1: structures of furan oligomers HOMO and LUMO (n = 1….9)

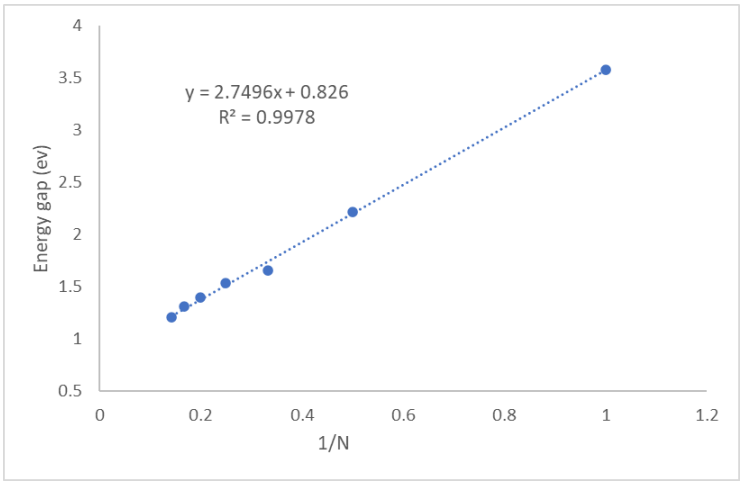

Fig. (7) shows the relationship between E gap and the number of furan oligomers units (N= 1….9)

6. Determination of Glass Transition Temperature with polyfuran by computation simulation

The glass transition temperature is a pivotal parameter that characterizes the thermal range within which polymers transition from the rigid glassy state to the more flexible rubbery state. This transformation markedly affects the mechanical, thermal, and viscoelastic properties of polymers, making Tg critical for applications related to polyfuran. Molecular dynamics simulations were employed to ascertain the magnitude of the influence of nanosized copper oxide on the degree of glass transition. As demonstrated in Figures (8,9), a significant increase in the glass transition temperature

was observed, ranging from (469 - 476.22) for PFu and Pfu@CuO NPs, respectively. These results align with the experimental findings acquired through differential scanning calorimetry (DSC), as illustrated in Figures (10,11). It was determined that the glass transition temperature escalated from 442℃ to 484 ℃ for PFu and Pfu@CuO NPs, respectively. The observed elevation in the glass transition temperature resulted from the limitation of polymer chain mobility. However, the utilization of computational simulation techniques is of considerable significance. Such simulations empower researchers to elucidate the dynamics of polymer chains at the molecular scale. Computational simulations present a cost-effective alternative to conventional experimental approaches, facilitating the rapid assessment of varied polymer compositions and conditions without necessitating extensive laboratory experimentation [39–40].

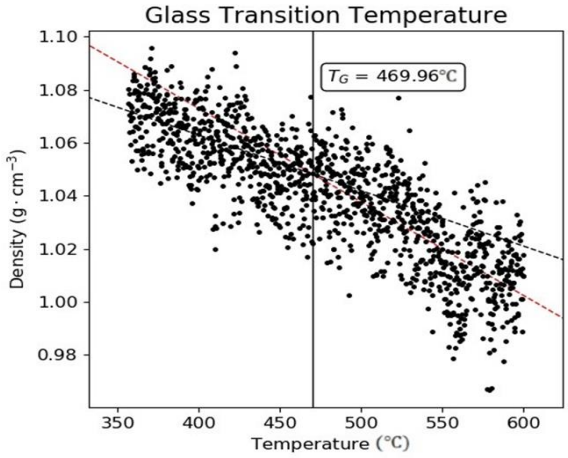

Fig. 8 Glass Transition Temperature with PFu. computation simulation

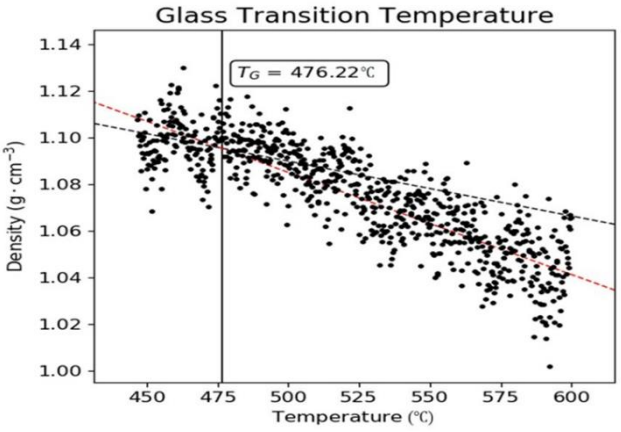

Fig. 9 Glass Transition Temperature with by PFu@CuO NPs by computation simulation

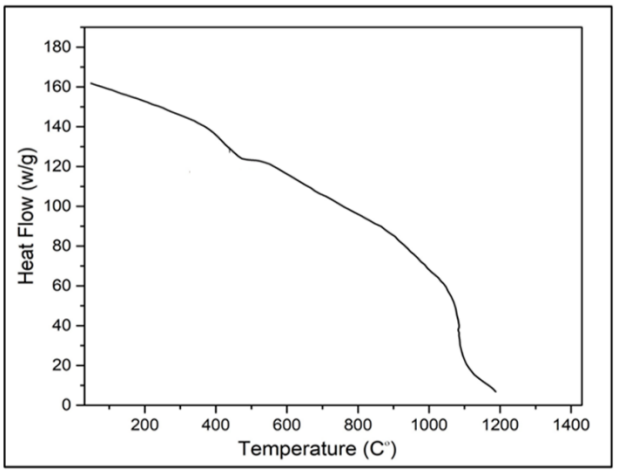

Fig.10 Glass Transition Temperature with polyfuran DSC.

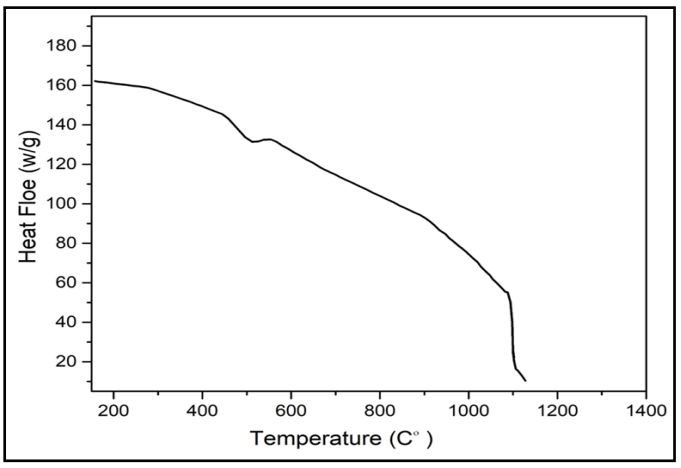

Fig.11 Glass Transition Temperature with by polyfuran by DSC.

3. Conclusion and future scope

Polyfuran and CuO nanoparticles (NPs) were efficiently synthesized via chemical oxidation polymerization and core-shell polymerization. Compared with PFu and PFu@CuO NPs, we notice a shift in the properties of the hybrid polymer prepared using copper oxide nanoparticles. A shift in the values of optical absorption lengths was observed, as well as an improvement in the morphology of the polymer through increased crystallinity and improved thermal stability. That is, intermolecular metal oxide nanoparticles play a crucial role in modifying the differences in polyfuran morphology during the polymerization process. The results of our study indicate. indicated that the morphology of poly

furans synthesized by chemical oxidative polymerization of the core shell could be easily modified by introducing a small amount of CuO nanoparticles. On the one hand, molecular dynamics simulations were used using density function theory (DFT), which included studying the effect of the number of monomers on the energy gap in the polymer chain. On the other hand, it was hoped to use molecular dynamic simulations to conduct theoretical calculations of the glass transition degree for polyfuran and polyfuran supported with nanosized copper oxide, which were compared with the experimentally calculated glass transition degree using differential calorimetry (DSC), which gave consistent results that demonstrated the effect of nanosized oxide on increasing the glass transition degree, which provides a way to For researchers to study the properties of polymers and potential future applications

Disclosure statement: *Conflict of Interest:* The authors declare no conflicts of interest.

Compliance with Ethical Standards: This article contains no studies involving human or animal subjects.

Reference

[1] Chan, W. K. (2007) Metal containing polymers with heterocyclic rigid main chains, *Coordination Chemistry Reviews*, 251(17-20), 2104-2118.

[2] Abd-El-Aziz, A., and Manners I., (2007) Frontiers in Transition Metal-Containing Polymers, *J. of Inorganic and Organometallic Polymers and Materials*. 17(4):687-688 .

[3] Khaudeyer, H. S., Kadhim, Z. N., & Hanoosh, W. S. (2015) Thermal stability of some new metal containing polymers based on resol-bisphenol a formaldehyde resin, *Research Journal of Science and Technology*, 7(3), 183-190 .

[4] Ninis, O., Abarkan, M., and Bouachrine, M.(2015) Combined experimental and theoretical study of structural and optoelectronic properties of Polyfuran with its oligomers. *IEEE 12th International Multi-Conference on Systems, Signals & Devices (SSD15). IEEE* .

[5] Argun, A. A., Aubert, P. H., Thompson, B. C., Schwendeman, I., Gaupp, C. L., Hwang, J. and Reynolds, J. R. (2004) Multicolored electrochromism in polymers: structures and devices, *Chemistry of materials*, 16(23), 4401-4412.

[6] Katz, H. E., and Bao, Z. (2000) The physical chemistry of organic field-effect transistors, *The Journal of Physical Chemistry B*, 104(4), 671-678.

[7] Grätzel, M. (2004) Conversion of sunlight to electric power by nanocrystalline dye-sensitized solarcells. Journal of Photochemistry and Photobiology, *A: Chemistry*, 164(1-3), 3-14. vol.7,2004, pp36-40.

[8] Liang, J., Ying, L., Yang, W., Peng, J., & Cao, Y. (2017) Improved efficiency of blue polymer light-emitting diodes using a hole transport material, *Journal of Materials Chemistry C*, 5(21), 5096-5101.

[9] Gidron, O. (2016) Oligofurans. Organic Redox Systems: Synthesis, Properties, and Applications, 445-462

[10] Dou, L., Liu, Y., Hong, Z., Li, G., & Yang, Y. (2015) Low-band gap near-IR conjugated polymers/molecules for organic electronics. Chemical, *reviews*, 115(23), 12633-12665 .

[11] Torsi, L., Magliulo, M., Manoli, K., & Palazzo, G. (2013) Organic field-effect transistor sensors: a tutorial,*chemical society review* ,22 .

[12] Thomas, S. W., Joly, G. D., & Swager, T. M. (2007) Chemical sensors based on amplifying fluorescent conjugated polymers, *Chemical reviews*, 107(4), 1339-1386.

[13] Pasini, D., & Zapotoczny, S. (2023). Synthesis, Processing and Applications of Conjugated Oligomers and Polymers 2.0. *International Journal of Molecular Sciences*, *24*(14), 11623.

[14] Chandrasekhar, P. (2018) Conducting polymers, fundamentals and applications , New York: Springer. p. 850

[15] González-Tejera, M. J., de la Blanca, E. S., and Carrillo, I. J. (2008) Polyfuran conducting polymers: Synthesis, properties, and applications, *Synthetic Metals*, 158(5), 165-189.

[16] Mumit, M. A., Pal, T. K., Alam, M. A., Islam, M. A. A. A. A., Paul, S., & Sheikh, M. C. (2020) DFT studies on vibrational and electronic spectra, HOMO–LUMO, MEP, HOMA, NBO and molecular docking analysis of benzyl-3-N-(2, 4, 5-tri methoxy phenylmethylene) hydrazinecarbodithioate, *Journal of molecular structure*, 1220, 128715.

[17] Ma, X., Chang, D., Zhao, C., Li, R., Huang, X., Zeng, Z, and Jia, Y. (2018) Geometric structures and electronic properties of the Bi 2 X 2 Y (X, Y= O, S, Se, and Te) ternary compound family: a systematic DFT study. *Journal of Materials Chemistry C*, 6(48), 13241-13249.

[18] Li, Xin-Gui, Yan Kang, and Mei-Rong Huang . (2006) Optimization of polymerization conditions of furan with aniline for variable conducting polymers, *Journal of combinatorial chemistry*, 8(5), 670-678 .

[19] Mirmohammadi, S. A., Imani, M., Uyama, H., & Atai, M. (2014) International Journal of Polymeric Materials and Polymeric Biomaterials 63: Hybrid organic-inorganic nanocomposites based on poly (epsilon)-caprolactone)/polyhedral oligomeric silsesquioxane: Synthesis and in vitro evaluations, *Cellular Polymers*, 33(6), 331-332.

[20] Alshawi, F. M., and Hanoosh, W. S., (2019) Synthesis and thermal properties of some phenolic resins, *Innova ciencia*, 7(1), 1-15 .

[21] Khaudeyer, H. S., Kadhim, Z. N., & Hanoosh, W. S. (2015). Thermal stability of some new metal containing polymers based on resol-bisphenol a formaldehyde resin. *Research Journal of Science and Technology*, *7*(3), 183-190.

[22] Şen, S., Bardakçı, B., Yavuz, A. G., & Gök, A. U. (2008) Polyfuran/zeolite LTA composites and adsorption properties, *European polymer journal*, 44(8), 2708-2717.
[23] Bajwa, A., Kumar, S., & Singh, G. (2024) Investigation of structural, optical & morphological characteristics of CuO nanoparticles synthesized via co-precipitation method, *In AIP Conference Proceedings* (Vol. 2986, No. 1). AIP Publishing.
[24] Radhakrishnan, A. A., & Beena, B. B. (2014) Structural and optical absorption analysis of CuO nanoparticles, *Indian J. Adv. Chem. Sci*, 2(2), 158-161.
[25] Zare, E. N., Lakouraj, M. M., Moghadam, P. N., & Azimi, R. (2013) Novel polyfuran/functionalized multiwalled carbon nanotubes composites with improved conductivity: Chemical synthesis, characterization, and antioxidant activity, *Polymer composites*, 34(5), 732-739.
[26] Hanoosh, W. S., & Abdelrazaq, E. M. (2009) Polydimethyl siloxane toughened epoxy resins: tensile strength and dynamic mechanical analysis. *Malaysian Polymer Journal*, 4(2), 52-61.
[27] Alakhras, F. and Holze, R., (2007) In situ UV–vis-and FT-IR-spectroscopy of electrochemically synthesized furan–thiophene copolymers, *Synthetic metals*, 157(2-3), 109-119.
[28] Nazarzadeh Z. E., Lakouraj, M. M., & Baghayeri, M. (2015) Electro-magnetic polyfuran/Fe3O4 nanocomposite: synthesis, characterization, antioxidant activity, and its application as a biosensor. International *Journal of Polymeric Materials and Polymeric Biomaterials*, 64(4), 175-183 .
[29] Cai, J., Yu, Q., Zhang, X., Lin, J., & Jiang, L. (2005) Control of thermal cross-linking reactions and the degree of crystallinity of syndiotactic 1, 2-polybutadiene. *Journal of Polymer Science Part B: Polymer Physics*, 43(20), 2885-2897.
[30] Al-Muntaser, A. A., Banoqitah, E., Morsi, M. A., Madkhli, A. Y., Abdulwahed, J. M., Alwafi, R., and Saeed, A., (2023) Fabrication and characterizations of nanocomposite flexible films of ZnO and polyvinyl chloride/poly (N-vinyl carbazole) polymers for dielectric capacitors. *Arabian Journal of Chemistry*, 16(10), 105171.
[31] Li, X. G., Li, J., Meng, Q. K., & Huang, M. R. (2009) Interfacial synthesis and widely controllable conductivity of polythiophene microparticles, *The Journal of Physical Chemistry B*, 113(29), 9718-9727.
[32] Cooper, T. G., & de Leeuw, N. H. (2004) A computer modeling study of the competitive adsorption of water and organic surfactants at surfaces of the mineral scheelite, *Langmuir*, 20(10), 3984-3994..
[33] Hiemenz, P. C., & Rajagopalan, R. (2016) Principles of Colloid and Surface Chemistry, revised and expanded. CRC press.
[34] Athal, M. A., Hanoosh, W. S., & Abdullah, A. Q. (2020). Analysis of band gap energy and refractive index of electrospinning polyacrylonitrile (PAN) nanofibers. *Basrah Journal of Science*, *38*(1), 111-130.
[35] Yasumura, S., Kamachi, T., Toyao, T., Shimizu, K. I. and Hinuma, Y. (2023) Prediction of stable surfaces of metal oxides through the unsaturated coordination index. *ACS omega*, 8(32), 29779-29788.
[36] Dereli, Ö., Sudha, S., & Sundaraganesan, N. (2011) Molecular structure and vibrational spectra of 4-phenylsemicarbazide by density functional method, *Journal of molecular structure*, 994(1-3), 379-386.
[37] Abood, N. A., Al-Askari, M., & Saeed, B. A. (2012). Structures and vibrational frequencies of imidazole, benzimidazole and its 2-alkyl derivatives determined by DFT calculations. *Basrah J. Sci*, *30*, 119-131.
[38] Saleh, B. A., Issa, A. Y., Al-Mowali, A. H., & Khalaf, M. N. Study of Substituent Effect on Band Gaps of Oligothiophene by Using Semi-Empirical Molecular Orbital Calculations.
[39] Alamfard, T., Lorenz, T., & Breitkopf, C. (2024). Glass Transition Temperatures and Thermal Conductivities of Polybutadiene Crosslinked with Randomly Distributed Sulfur Chains Using Molecular Dynamic Simulation. *Polymers*, *16*(3), 384.
[40] Sarangapani, R., Reddy, S. T., & Sikder, A. K. (2015). Molecular dynamics simulations to calculate glass transition temperature and elastic constants of novel polyethers. *Journal of Molecular Graphics and Modelling*, *57*, 114-121.